# The effect of Boron on the doping efficiency of Nitrogen in ZnO

**Article** *in* Journal of Alloys and Compounds · February 2016

DOI: 10.1016/j.jallcom.2016.02.147



Xingyou Chen
Chinese Academy of Sciences



Yong-gang Zhang
Chinese Academy of SciencesSIMITShanghai



Yi Gu
Stony Brook University

Journal of Alloys and Compounds 672 (2016) 260–264

Contents lists available at ScienceDirect

Journal of Alloys and Compounds

journal homepage: http://www.elsevier.com/locate/jalcom

# The effect of boron on the doping efficiency of nitrogen in ZnO

Xingyou Chen [a, b], Zhenzhong Zhang [a, *], Bin Yao [c, **], Yonggang Zhang [b], Yi Gu [b], Pengcheng Zhao [a], Binghui Li [a], Dezhen Shen [a]

[a] State Key Laboratory of Luminescence and Applications, Changchun Institute of Optics, Fine Mechanics and Physics, Chinese Academy of Sciences, Changchun 130033, PR China
[b] State Key Laboratory of Function Materials for Informatics, Shanghai Institute of Microsystem and Information Technology, Chinese Academy of Sciences, Shanghai 200050, PR China
[c] State Key Laboratory of Superhard Materials and College of Physics, Jilin University, Changchun 130023, PR China

ARTICLE INFO

*Article history:*
Received 14 December 2015
Received in revised form
4 February 2016
Accepted 16 February 2016
Available online 18 February 2016

*Keywords:*
Zinc oxide
Molecular beam epitaxy
Boron–nitrogen codoping
Hall-effect
X-ray photoelectron spectra
Photoluminescence

ABSTRACT

Stable p-type boron–nitrogen codoped ZnO thin films were prepared by plasma-assisted molecular beam epitaxy. The incorporations of boron and nitrogen into ZnO, identified by X-ray diffraction and X-ray photoelectron spectroscopy, led to improvement in p-type conductivity of ZnO with respect to nitrogen monodoped ZnO. It was ascribed to the marked enhancement of nitrogen doping efficiency due to the existence of two types of chemical states of nitrogen atoms: the nitrogen substituting at oxygen site with nearest neighbor of Zinc atom ($N_O$–Zn bonding), and the nitrogen locating at the nearest neighbor of boron atom ($N_O$–B bonding). The strong interaction between the boron and nitrogen makes the complex of $B_{Zn}$-$nN_O$ ($n$ = 3 or 4) be a shallow acceptor, which is responsible for the observed p-type behavior.



## 1. Introduction

The II–VI compound semiconductor, ZnO, is particularly interesting because of wide direct band gap of 3.37 eV at room temperature and large exciton binding energy of 60 meV. However, its potential for applications in blue and UV solid-state lighting devices and photodetectors has been impeded by the difficulty of achieving p-type ZnO for many years [1–3]. Nitrogen (N), as a promising p type dopant in ZnO, has been investigated deeply during the last decade, because its electronic structure and its ionic radius are closer to that of oxygen. Although a theoretical report predicted that nitrogen on an oxygen site ($N_O$) is a deep acceptor [4–6], many p-type results were achieved by N doping. And a subsequent theoretical report demonstrated p-type N-doped ZnO can be realized by forming a shallow acceptor of $N_O$–$V_{Zn}$ [11,12]. However, due to the weaker chemical stability of nitrogen in ZnO than some metal impurity in semiconductors (eg. Mg in GaN), N doped ZnO is suffering from relatively low hole concentration, low hole mobility, and most of all low reproducibility [7–10]. Codoping method, using acceptor (e.g. N) and donor (e.g. boron, aluminum, gallium or indium) simultaneously, has been also proposed to enhance the incorporation of acceptors and lower its ionization energy through the strong attractive interactions between acceptor and donor [13–15]. Researches of N codoping with aluminum (Al), gallium (Ga) and indium (In) have been reported with varied degrees of success [16–18]. So far boron–nitrogen (B–N) codoping method by using molecular beam epitaxy (MBE) has rarely been reported due to the absence of high purity B source [19]. Sui et al. found that B–N co-doping can obtain p-type ZnO (ZnO:(B, N)) by magnetron sputtering and annealing [20]. But, boron atom state in ZnO and the doping mechanism are still not clear.

In this work, p-type ZnO thin films prepared using N monodoping and B–N codoping method by plasma-assisted molecular beam epitaxy (P-MBE) technique were investigated comparatively. Compared to ZnO:N, the ZnO:(B, N) showed higher hole concentration and lower resistivity with better stability. The effect of incorporation of B atom on the N doping efficiency in ZnO was discussed.

* Corresponding author.
** Corresponding author.
*E-mail addresses:* exciton@163.com (Z. Zhang), binyao@jlu.edu.cn (B. Yao).

http://dx.doi.org/10.1016/j.jallcom.2016.02.147
0925-8388/

## 2. Experimental details

The ZnO thin films studied in this paper were grown by VG V80H P-MBE. It has been demonstrated that *a*-plane sapphire (*a*-$Al_2O_3$) is helpful in reducing the residual electron concentration of the ZnO films in our previous paper [21]. Thus, *a*-plane sapphire has been employed as substrate for the growth. The substrate was cleaned in an ultrasonic bath in acetone for 10 min and ethanol for 5 min, followed by de-ionized water rinsing for 5 min. Then the substrate was etched in a mixed solution of $H_2SO_4$:$H_3PO_4$ = 3:1 at 160 °C for 15 min. Finally the substrate was washed with de-ionized water and blown dried using nitrogen gas. After chemical cleaning and etching, the substrate was heated at about 600 °C for 30 min in a preparation chamber to remove possible adsorbed surface contamination. Then it was sent into the growth chamber. 6N-purity zinc (Zn) held in a Knudsen effusion cell was used as Zn source. Highly purity hexagonal boron nitride (*h*-BN) ceramic lining was activated by 5N-purity nitric oxide (NO) in an Oxford Applied Research Model HD 25 radio-frequency (13.56 MHz) plasma source to generate O precursor, N and B dopants simultaneously for the codoping of ZnO. By changing the NO flux in a range of 1.2 to 0.6 SCCM (Standard Cubic Centimeters per Minute), a series of samples were fabricated and defined as *a*, *a1*, *a2*, and *a3*, respectively, as shown in Table 1. The RF power was adjusted to control the numbers of species of N and B in the plasma. By replacing the *h*-BN ceramic lining with a quartz sleeve, the ZnO:N thin film can also be fabricated under the same condition. Before growth, the substrate was treated again by O plasma at 500 °C for 15 min to remove the contaminant carbon adsorbed on the surface of the substrate, then the substrate temperature was decreased and kept at 450 °C. During the growth process, the order of magnitude for the pressure in the growth chamber was maintained at about $10^{-5}$ mbar and a growth rate of about 200 nm/h was used for the epilayer growth. A ZnO:N thin film (defined as sample *b*) and a nominally undoped ZnO thin film (defined as sample *c*), were also grown under the same growth temperature and pressure for comparison.

Electrical properties of the films were measured in a Hall measurement system (Lakeshore 7707) under Van der Pauw configuration. Crystal structures of the films were studied with Bruker D8 GADDS X-ray diffraction using Cu Ka ($\lambda$ = 0.15406 nm) as the excitation source. X-ray photoelectron spectra (XPS) (Thermo ESCALAB 250, Al K$\alpha$ radiation source $h\nu$ = 1486.6 eV) were measured to study the chemical states of the doped elements. The absorption spectra of the thin films were recorded in a Shimadzu UV-3101PC scanning spectrophotometer. Low-temperature photoluminescence (PL) measurements were performed by using the Jobin–Yvon UV Lab Ram Infinity Spectrophotometer with He–Cd laser line of 325 nm as an excitation source.

## 3. Results and discussion

### 3.1. Electrical measurements

The typical thickness of this group of samples is about 600 nm. Their electrical properties were obtained at room temperature by the four-probe van der Pauw method using HMS7707 Hall-effect measurement system. Before measurements, four In spot electrodes were made at the four corners of a square sample (5 × 5 $mm^2$) and the ohmic contact between electrodes and films was confirmed. Results of Hall probe analysis on the films are shown in Table 1. To confirm further the conduction type, the measurements were performed on various magnetic fields from 3 to 15 KGauss with a step of 3 KGauss. Every set of data at a certain magnetic field were obtained from averaging outputs under four contact configurations (electrodes 1,2 injection and 4,3 measure, similarly 2,3/1,4, 3,4/2,1 and 4,1/3,2) and positive–negative current injections. The nominally undoped ZnO showed n-type with an electron concentration in the order of magnitude of $10^{17}$ $cm^{-3}$. Many literature found the window of the deposition parameters for achieving p-type ZnO through N doping was very narrow [8,16,22], and Hall effect measurement usually revealed an inferior p-type conduction with relatively low hole concentration (~$10^{17}$ $cm^{-3}$) and low hole mobility (~$10^{-1}$ $cm^2$ $V^{-1}$ $S^{-1}$). This means not all of those N atoms acted efficient acceptors at room temperature. Whereas in this experiment, p-type behaviors could observed for almost all the ZnO:(B, N) thin films deposited at temperatures in the range of 350–550 °C, with a higher hole concentration of $10^{17}$–$10^{18}$ $cm^{-3}$, a lower resistivity of 1–10 Ω cm and a relatively higher carrier mobility of 1–6.3 $cm^2$ $V^{-1}$ $S^{-1}$, as shown in Table 1, which could be comparable to the dual-acceptor doping results [23]. Moreover, the p-type conduction shows no marked degradation during the storage period of more than two years. During the preservation period of time, the carrier density drops a little in the first several days and then fluctuates slightly. The time-dependent electrical property is much the same as the tendency shown in the Ref. [19]. These results demonstrated that the B–N codoping method is an effective approach to achieve stable p-type ZnO.

### 3.2. X-ray photoelectron spectra

To identify the chemical states of B and N in the ZnO:(B, N) thin films, XPS measurement was performed for sample *a* after $Ar^+$ etching the surface of the film. Fig. 1(a) and (b) show typical N 1*s* and B 1*s* XPS spectra of the ZnO:(B, N) respectively, demonstrating incorporation of both B and N into ZnO. As shown in Fig. 1(a), two XPS peaks are observed, one locates at the binding energy of 396 eV, it also appears in the XPS spectrum of ZnO:N and is attributed to N in Zn–N bond [24], meaning N substituting at O site to act as a acceptor. And another peak locates at the binding energy of 399.4 eV, which could be considered to be N in B–N bond, because it is similar to the reported position of the N 1*s* spectrum (399 eV) of B–N bond in h-BN [25,26]. Moreover, a sharp peak locates near the binding energy of 191.3 eV in the B 1*s* spectrum in Fig. 1(b), which is very close to the 1s core level at 191.5 eV of B in BN with hexagonal phase [27]. In addition, an intense and broad peak centering at around 198.8 eV is also observed on the high energy side of the B 1*s* spectrum. Both of these two peaks are similarly to the previously reported position of the B 1s spectrum of

**Table 1**
Electrical properties of thin films deposited under different growth regimes ($T_d$ = 450 °C).

| Sample | Doping Source | NO Flux (SCCM) | $O_2$ Flux (SCCM) | RF Power (W) | Resistivity (Ω cm) | Hall Mobility ($cm^2$ $V^{-1}$ $S^{-1}$) | Carrier Concentration ($cm^{-3}$) | Carrier Type |
|---|---|---|---|---|---|---|---|---|
| *a* | B, N | 0.6 | | 280 | 2.9 | 2.2 | 9.5 × $10^{17}$ | p |
| *a1* | B, N | 1.2 | | 250 | 5.5 | 6.3 | 1.8 × $10^{17}$ | p |
| *a2* | B, N | 0.9 | | 250 | 2.2 | 1.8 | 1.6 × $10^{18}$ | p |
| *a3* | B, N | 0.6 | | 250 | 2.0 | 1.0 | 3.0 × $10^{18}$ | P |
| *b* | N | 0.6 | | 280 | 186 | 0.3 | 1.3 × $10^{17}$ | weak p |
| *c* | undoped | | 0.6 | 280 | 14.4 | 1.2 | 3.6 × $10^{17}$ | n |

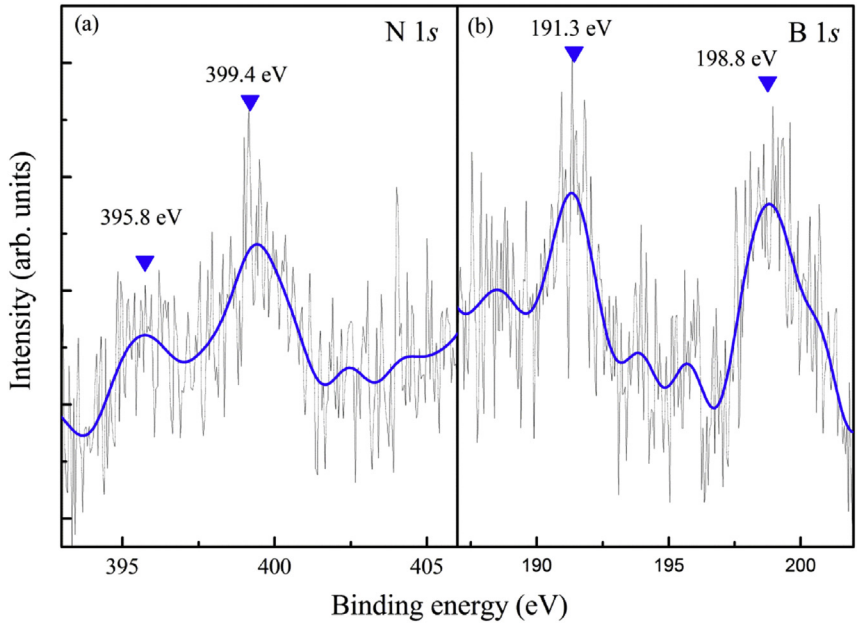


**Fig. 1.** XPS spectrum of (a) N 1s and (b) B 1s core level of the ZnO:(B, N) produced with NO flux of 0.6 SCCM and power of 280 W, respectively.

BN examined by XANES or EELS spectra [28–30], implying that B atoms were incorporated in ZnO lattice. Both the B 1*s* and the N 1*s* spectra clearly indicate the existence of configurations of B–N and Zn–N bonds in ZnO lattice. In addition, it is noted that no specific peak is observed near the region of 193.0 eV, corresponding to the binding energy of B 1*s* of B–O bond in $B_2O_3$ [29], which means that most of the nearest neighbor sites of B atoms are occupied by N atoms rather than O atoms. Considering that the B doping was realized by plasma bombarding the BN lining, the dopant may be B–N3 or B–N4 clusters. Furthermore, the high B–N bond energy ensures the stability of B–N bond during the thin film growth. In this case, B atom bared in O atom neighbors can be neglected, although boron at Zn site ($B_{Zn}$) acting as a weak donor in ZnO according to the literature [29]. Based on the codoping theory [12], it would be reasonable to believe that there exists acceptor complex of $B_{Zn}$-$n$$N_O$ ($n = 3$ or 4) besides the deep $N_O$ acceptor. As a weak donor in ZnO, B atom has no occupied *d* orbital and low *p* orbital energy, so the defect ionization energy level of $B_{Zn}$-$n$$N_O$ should be lower than that of $N_O$ due to smaller cation *p* and anion *p* coupling [13,31]. The theoretical analysis has also revealed shallower levels and stabler chemical state of acceptor in ZnO:(B, N) with respect to that in ZnO:N [32]. Therefore, the B–N bond not only enhances the incorporation of N atoms, but also decreases the $N_O$ acceptor level depth in the band gap of ZnO. The acceptor complex $B_{Zn}$-$n$$N_O$ is responsible for the observed high hole concentration in ZnO:(B, N) at room temperature.

### 3.3. Structural properties

Fig. 2 shows two typical normalized XRD θ–2θ patterns of the B–N codoped (sample *a*) and nominally undoped ZnO (sample *c*) films. Besides the diffraction peak of $Al_2O_3$ (110), only ZnO (002) peak is observed for the two samples and no other phases (e.g., $B_2O_3$, BN, or $Zn_3N_2$) are detected, indicating that the samples crystallize in wurtzite structure with a high c-axis preferred orientation. It is noted that the diffraction angle (2θ) of the (002) peak is 34.41° for the ZnO:(B, N) film, which is larger than that of undoped ZnO (34.34°). Since the B–N bond length either in *h*-BN (1.42 Å) or *c*-BN (1.57 Å) structure [33,34] is smaller than those of

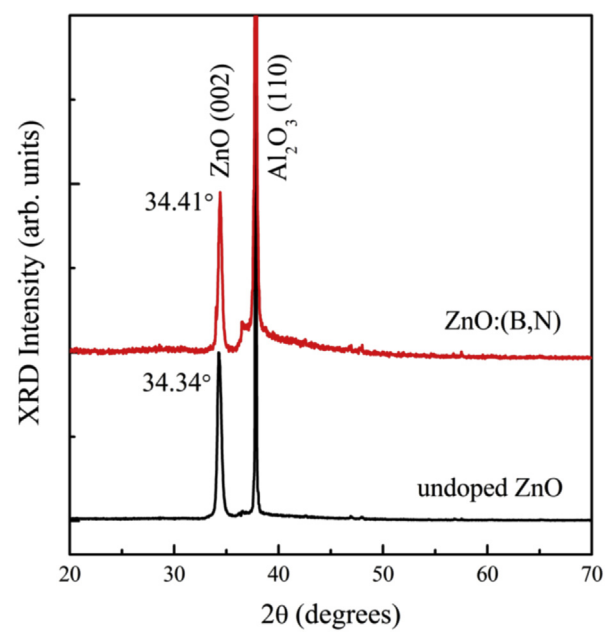


**Fig. 2.** XRD θ–2θ patterns of the undoped ZnO and ZnO:(B, N) produced with NO flux of 0.6 SCCM and power of 280 W.

Zn–O (1.93 Å) or Zn–N (1.88 Å) [35], and the effect of substitution of N for O on the lattice constant of ZnO in c-axis is little [36], thus the diffraction angle shift of (002) peak for the ZnO:(B, N) film is mainly due to the formation of B–N bond.

### 3.4. Absorption spectra

To study the influence of B–N codoping on the optical band gap of ZnO, the B–N codoped (sample *a*), N-doped (sample *b*) and nominally undoped (sample *c*) ZnO thin films are investigated by using optical absorption spectra recorded at room temperature. All the samples show the transmittance over 90% in the visible region.

The absorption coefficient ($\alpha$) is obtained from the absorption spectra. According to the photoelectric equation, $(\alpha h\nu)^2 = C(h\nu - E_g)$, where $\alpha$ and $E_g$ is the absorption coefficient and optical bandgap of ZnO respectively, $h\nu$ is the photon energy of incident light, and $C$ is a constant. The optical band gaps of these three samples could be derived from a plot of $(\alpha h\nu)^2$ as a function of photon energy $h\nu$ [37]. That is, using extrapolation method, the value in X axis of intersection point of the tangent line of the curve is the energy of optical absorption edge, as shown in Fig. 3. The absorption edge of the ZnO:N film shows a little redshift compared to the nominally undoped ZnO film, meaning that the optical band gap has been narrowed after N-doping mainly due to the overlap between the acceptor defect levels and band gap tails [38], as shown in Fig. 3. On the contrary, the optical band gap of ZnO:(B, N) broadens about 30 meV compared to that of ZnO:N. This blueshift should be associated with the incorporation of B into ZnO lattice.

### 3.5. Optical properties

To have a deep understanding of the influence of incorporation of B and N atoms on the optical properties of the ZnO:(B, N), a low temperature (80 K) PL comparison with the ZnO:N sample was performed which is shown in Fig. 4. The spectrum of the N-doped sample is dominated by a neutral donor-bound exciton (D°X) at 3.363 eV, which appears frequently in doped or nominally undoped ZnO [39,40]. The donor usually is attributed to the shallow donors of native defects (such as zinc interstitial $Zn_i$) [41] or impurities (such as H) [42,43], which is considered as the main obstacle for p-type doping of ZnO. Especially for the incorporation and diffusivity of H, it is always unavoidable in the growing process of ZnO. On the low energy side, a peak centered at 3.325 eV is often assigned to the free electron to acceptor (FA) transition which normally appears in ZnO:N samples [44]. In addition, a line locates at about 3.253 eV, with two gradually weaker shoulders centered at 3.191 and 3.119 eV, respectively are assigned to the recombination of donor–acceptor pair (DAP) [44], and DAP-LO, and DAP-2LO replica, respectively [45]. Similarly, the peak located at 3.253 eV in the spectrum of ZnO:(B, N) sample, can also be classified as a DAP transition, as shown in Fig. 4. By comparing with the spectrum of ZnO:N, the major features observed in the PL spectrum of ZnO:(B, N) are a broad peak at 3.403 eV, but no other details are observed in the D°X region. Moreover, the peak located at 3.403 eV shows an about 30 meV blueshift with respect to the free exciton (FE) peak of ZnO single crystal [40], which agrees well with the shift of optical absorption edge. Therefore, this peak should still come from the FE peak, while the blueshift of FE peak probably results from a wider band gap of B–N codoped ZnO than that of ZnO [46–48].

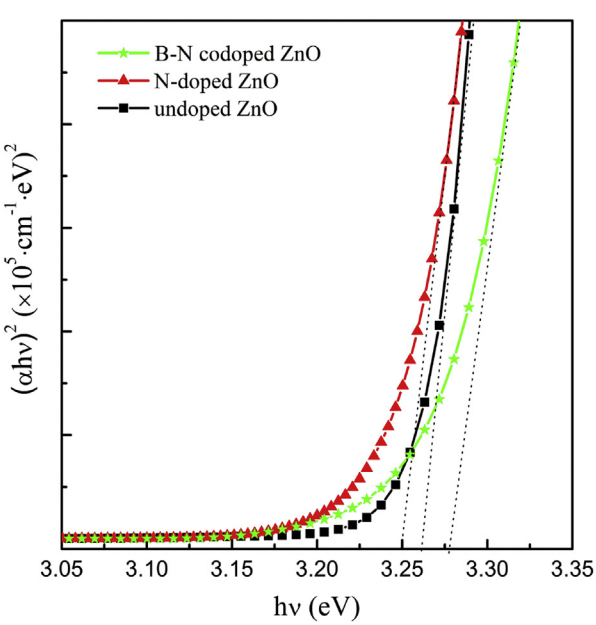


**Fig. 3.** Optical absorption spectra of the undoped ZnO, ZnO:N and ZnO:(B, N) produced with NO flux of 0.6 SCCM and power of 280 W.

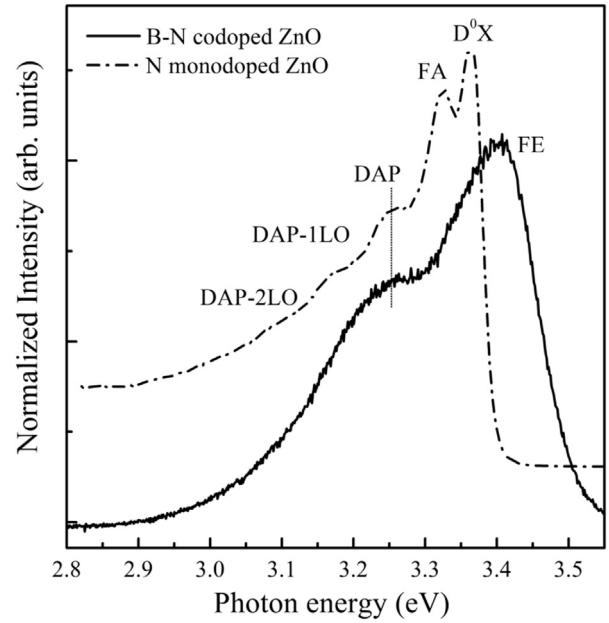


**Fig. 4.** Normalized 80 K PL spectra of the ZnO:N and ZnO:(B, N) produced with NO flux of 0.6 SCCM and power of 280 W.

Based on the above analyses, the B–N codoping method has enhanced the N-doping efficiency markedly. Compared to ZnO:N, there are two types of chemical states of N atoms in the ZnO:(B, N): One is the $N_O$ with the nearest neighbor of Zn atom, corresponding to a deep acceptor, and the other one is the $N_O$ with the nearest neighbor of B atom, which is a shallow acceptor with a configuration of $B_{Zn}$-$nN_O$ ($n = 3$ or 4) and drives the high hole concentration in the ZnO:(B, N) thin films. To check the p-type conductivity, further works on the fabrication of homojunction light emitting diode based on ZnO:(B, N) are ongoing.

## 4. Conclusion

In summary, high hole concentration and low resistivity p-type ZnO:(B, N) thin films have been fabricated by using P-MBE technique through B–N codoping method. The introductions of B and N atoms into ZnO lattice were both identified. In comparison to the nitrogen monodoping method, the B–N codoping method expanded the deposition window for achieving p-type conduction due to the high B–N bond energy. Moreover, the incorporation of B blueshifted the band edge of ZnO. B–N codoping may be a promising way to produce p-type ZnO.

## Acknowledgment

This work is supported by the Key Program of the National Natural Science Foundation of China (11134009), the National Natural Science Foundation of China under Grant Nos. (11174273, 11104265, 61376054, 11274135) the 100 Talents Program of the

Chinese Academy of Sciences.

## References


[1] Z.K. Tang, G.K.L. Wong, P. Yu, Appl. Phys. Lett. 72 (25) (1998) 3270.
[2] D.M. Bagnall, Y.F. Chen, Z. Zhu, T. Yao, Appl. Phys. Lett. 73 (8) (1998) 1038.
[3] T. Makino, C.H. Chia, T.T. Nguen, Y. Segawa, Appl. Phys. Lett. 77 (11) (2000) 1632.
[4] J.L. Lyons, A. Janotti, C.G. Van de Walle, Appl. Phys. Lett. 95 (2009) 252105.
[5] M.C. Tarun, M. Zafar Iqbal, M.D. McCluskey, AIP Adv. 1 (2011) 022105.
[6] M.D. McCluskey, C.D. Corolewski, J.P. Lv, M.C. Tarun, S.T. Teklemichael, E.D. Walter, M.G. Norton, K.W. Harrison, S. Ha, J. Appl. Phys. 117 (2015) 112802.
[7] T.M. Barnes, K. Olson, C.A. Wolden, Appl. Phys. Lett. 86 (2005) 112112.
[8] X. Li, Y. Yan, T.A. Gessert, C. Dehart, C.L. Perkins, D. Young, T.J. Coutts, Electrochem. Solid State 6 (2003) C56.
[9] X.L. Guo, H. Tabata, T. Kawai, J. Cryst. Growth 223 (2001) 135.
[10] A.B.M.A. Ashrafi, I. Suemune, H. Kumano, S. Tanaka, Jpn. J. Appl. Phys. 41 (2002) L1281.
[11] L. Liu, J.L. Xu, D.D. Wang, M.M. Jiang, S.P. Wang, B.H. Li, Z.Z. Zhang, D.X. Zhao, C.X. Shan, B. Yao, D.Z. Shen, Phys. Rev. Lett. 108 (2012) 215501.
[12] J.G. Reynolds, C.L. Reynolds, A. Mohanta, J.F. Muth, J.E. Rowe, H.O. Everitt, D.E. Aspnes, Appl. Phys. Lett. 102 (2013) 152114.
[13] T. Yamamoto, H. Katayama-Yoshida, Jpn. J. Appl. Phys. 38 (1999) L166;
a) T. Yamamoto, Phys. Stat. Sol. A 193 (3) (2002) 423;
b) T. Yamamoto, Jpn. J. Appl. Phys. 42 (2003) 514.
[14] M. Joseph, H. Tabata, T. Kawai, Jpn. J. Appl. Phys. 38 (1999) L1205.
[15] M. Joseph, H. Tabata, H. Saeki, K. Ueda, T. Kawai, Phys. B 302 (2001) 140–148.
[16] G.D. Yuan, Z.Z. Ye, L.P. Zhu, Q. Qian, B.H. Zhao, R.X. Fan, C.L. Perkins, S.B. Zhang, Appl. Phys. Lett. 86 (2005) 202106.
[17] K. Nakahara, H. Takasu, P. Fon, A. Yamada, K. Iwata, K. Matsubara, R. Hunger, S. Niki, J. Cryst. Growth 503 (2002) 237–239.
[18] J.M. Bian, X.M. Li, X.D. Gao, W.D. Yu, L.D. Chen, Appl. Phys. Lett. 84 (2004) 541.
[19] P.C. Zhao, Z.Z. Zhang, B. Yao, B.H. Li, S.P. Wang, M.M. Jiang, D.X. Zhao, C.X. Shan, L. Liu, D.Z. Shen, Chin. J. Lumin 35 (7) (2014) 795–799.
[20] Y.R. Sui, B. Yao, J.H. Yang, L.L. Gao, T. Yang, R. Deng, J. Lumin. 130 (2010) 1101–1105.
[21] J.S. Liu, C.X. Shan, S.P. Wang, F. Sun, B. Yao, D.Z. Shen, J. Cryst. Growth 312 (2010) 2861–2864.
[22] A. Tsukazaki, A. Ohtomo, T. Onuma, M. Ohtani, T. Makino, M. Sumiya, K. Ohtani, S.F. Chichibu, S. Fuke, Y. Segawa, H. Ohno, H. Koinuma, M. Kawasaki, Nat. Mater 4 (2005) 42.
[23] T.H. Vlasenflin, M. Tanaka, Solid State Commun. 142 (2007) 292–294.
[24] C.L. Perkins, S.-H. Lee, X. Li, S.E. Asher, T.J. Coutts, J. Appl. Phys. 97 (2005) 034907.
[25] M. Terrones, W.K. Hsu, H. Terrones, J.P. Zhang, S. Ramos, J.P. Hare, R. Castlllo, K. Prassldes, A.K. Cheetham, H.W. Kroto, D.R.M. Walton, Chem. Phys. Lett. 259 (1996) 568–573.
[26] J.F. Moulder, W.F. Stickle, P.E. Sobol, K.D. Bombem, in: J. Chastain (Ed.), Handbook of X-ray Photoeletron Spectroscopy, Perkin Elmer Co., Eden Prairie, MN, 1992.
[27] M. Bystrzejewski, A. Bachmatiuk, J. Thomas, P. Ayala, H.-W. Huebers, T. Gemming, E. Borowiak-Palen, T. Pichler, R.J. Kalenczuk, B. Büchner, M.H. Rümmeli, Phys. Status Solidi RRL 3 (2009) 193.
[28] K.S. Park, D.Y. Lee, K.J. Kim, D.W. Moon, Appl. Phys. Lett. 70 (1997) 315.
[29] L.J. Liu, T.K. Sham, W.Q. Han, Phys. Chem. Chem. Phys. 15 (2013) 6929.
[30] L. Song, L. Ci, H. Lu, P.B. Sorokin, C. Jin, J. Ni, et al., Nano Lett. 10 (2010) 3209–3215.
[31] J.B. Li, S.H. Wei, S.S. Li, J.B. Xia, Phys. Rev. B 74 (2006) 081201 (R).
[32] B. Deng, H.Q. Sun, Z.Y. Guo, X.Q. Gao, Acta Phys. Sin. 59 (2010) 1212–1218.
[33] M. Menon, D. Srivastava, Chem. Phys. Lett. 307 (1999) 407–412.
[34] O. Hod, J. Chem, Theory Comput. 8 (2012) 1360–1369.
[35] C.H. Park, S.B. Zhang, S.Hi Wei, Phys. Rev. B 66 (2002) 073202.
[36] B. Yao, D.Z. Shen, Z.Z. Zhang, X.H. Wang, Z.P. Wei, B.H. Li, Y.M. Lv, X.W. Fan, L.X. Guan, G.Z. Xing, C.X. Cong, Y.P. Xie, J. Appl. Phys. 99 (2006) 123510.
[37] S. Han, D.Z. Shen, J.Y. Zhang, Y.M. Zhao, D.Y. Jiang, Z.G. Ju, D.X. Zhao, B. Yao, J. Alloys. Comp. 485 (2009) 794–797.
[38] Z. Xu, Q.R. Zheng, G. Su, Phys. Rev. B 85 (2012) 075402.
[39] D.C. Look, D.C. Reynolds, C.W. Litton, R.L. Jones, D.B. Eason, G. Cantwell, Appl. Phys. Lett. 81 (10) (2002) 1830.
[40] B.Y. Zhang, B. Yao, S.P. Wang, Y.F. Li, C.X. Shan, J.Y. Zhang, B.H. Li, Z.Z. Zhang, D.Z. Shen, J. Alloys. Comp. 503 (2010) 155–158.
[41] D.C. Look, J.W. Hemsky, J.R. Sizelove, Phys. Rev. Lett. 82 (1999) 2552.
[42] C.G. Van de Walle, Phys. Rev. Lett. 85 (2000) 1012.
[43] D.M. Hofmann, A. Hofstaetter, F. Leiter, H.J. Zhou, F. Henecker, B.K. Meyer, Phys. Rev. Lett. 88 (2002) 045504.
[44] J.W. Sun, Y.M. Lu, Y.C. Liu, D.Z. Shen, Z.Z. Zhang, B. Yao, B.H. Li, J.Y. Zhang, D.X. Zhao, X.W. Fan, J. Appl. Phys. 102 (2007) 043522.
[45] F. Decremps, J. Pellicer-Porres, A.M. Saitta, J.-C. Cheervin, A. Polian, Phys. Rev. B 65 (2002) 092101.
[46] A. Zunger, A. Katzir, A. Halperin, Phys. Rev. B 13 (1976) 5560.
[47] C.H. Park, D.J. Chadi, Phys. Rev. B 55 (1997) 12995.
[48] K. Watanabe, T. Taniguchi, H. Kanda, Nat. Mater 3 (2004) 404.